



Semnan University

Mechanics of Advanced Composite Structures

journal homepage: <http://MACS.journals.semnan.ac.ir>

Study of High-cycle Fatigue Properties in Bovine Tibia Bones based on Reliability and Scatter-band Predictions

M. Farzannasab, M. Azadi*, H. Bahmanabadi

Faculty of Mechanical Engineering, Semnan University, Semnan, 351311911, Iran

KEYWORDS

Scatter-band
Reliability
High-cycle fatigue
Tibia bovine bone
Loading frequency

ABSTRACT

Bones are natural composites, which are consisted of mineral fibers, which strengthen the organic matrix. Such composites are exposed to both monotonic and cyclic loadings, which could predispose the structure to failure. One such failure mechanism could be the fatigue phenomenon. In this article, the scatter-band and the reliability response of bovine tibia bones were predicted in the load-controlled fatigue condition. The one-point rotary-bending fatigue machine was utilized to carry out standard tests at two different loading levels, 0.4 and 0.6 kg for three various loading frequencies, 10, 20 and 30 Hz for tibia bones. For scatter-band predictions, three confidence levels (85, 90, and 95%) were selected. Additionally, lower/upper bands were drawn for a selected target function, including the ratio of logarithmic fatigue lifetimes to stress levels. For the reliability prediction, three different distribution functions were considered. Results showed that, by decreasing the confidence level, the scatter-band would be narrower. Besides, the Probability of failure generally increased at 0.6 kg of the loading level, when the loading frequency increased.

1. Introduction

Bones could be considered as composite materials, which include mineral fibers, with high elastic modulus, which reinforce the organic matrix, with low elastic modulus [1]. Bones, as natural composites, have been exposed to various conditions such as monotonic and cyclic loadings, which cause the fatigue phenomenon. For engineers, such a topic is important in biomechanics to understand the fatigue behavior of human structures. It is also essential in understanding human bone pathologies and would be helpful in the prevention or diagnosis of such pathologies [2-5]. For this objective, fatigue tests have been performed on samples. However, related results usually have had remarkable scatter-bands, due to the lack of repeatability of testing. In addition, the reliability study of bone structures could be essential in finding appropriate alternative materials. In this field of study, some articles have been presented, which can be found in detail in the following paragraphs. The literature review was categorized into

two groups. One group was about bones and the other group was about the reliability analysis, particularly on bones.

For example, Carpinteri et al. [6] showed that bone failure occurred in a brittle manner and the load capacity of bones was limited up to a certain extent. Additionally, Kruzica and Ritchie [7] investigated the effect of age and disease conditions on fatigue and fracture characteristics of cortical bones. In another study, Tanner et al. [8] studied failures in bones, especially fatigue failures, which could be considered to be a precipitating factor in aseptic loosening of cemented joint replacements. Swanson et al. [9] studied fatigue properties of human cortical bones. They performed rotating cantilever fatigue tests on specimens extracted longitudinally from cortices of the human femur bones. Then, they found the usual inverse relationship between the stress amplitude and the fatigue lifetime. Carter et al. [10] examined the fatigue lifetime of compact bones and investigated the effect of the microstructure and density. They

* Corresponding author. Tel.: +98-910-2107280
E-mail address: m_azadi@semnan.ac.ir

proved that there was a significant positive correlation between the density and fatigue lifetime.

Moreover, Taylor [11] revealed that the effect of the specimen size on the fatigue lifetime was significant, based on the Weibull analysis and measuring the fatigue strength of bones. Carter and Caler [12] studied the effect of the physical characteristics of a tissue on uniaxial fatigue properties of human cortical bones. Their results indicated that the scatter-band was more pronounced in plots of the stress range versus the lifetime, than in ones of the strain range versus the lifetime. Turner et al. [13] investigated shear fatigue properties of human cortical bones, based on torsion testing. They showed that cortical bones exhibited superior fatigue properties under bending than those of tensile or compressive loading and had lower scatter-bands. Klemenc and Fajdiga [14] presented an estimation of the S-N curve and its scatter-band. They applied the two-parameter Weibull distribution to demonstrate the scatter-band of the lifetime at a particular stress level. In another publication, Rathod et al. [15] introduced a method for modeling the probabilistic distribution of the fatigue damage for single and multi-stress level loadings. They predicted the reliability by the proposed method, using the dynamic statistical model of the cumulative fatigue damage. Also, Schijve [16] compared three statistical distribution functions for the logarithmic lifetime. Their results depicted that the second function and the third function had a good agreement with the fitted data for 30 similar test results. Kobayashi et al. [17] evaluated the reliability in the volumetric measurement of bone defects. They indicated that errors of values between calculated and actual bone defects created in pig bones were up to 7.6%.

Furthermore, besides bone structures, fatigue properties of other composite types have been predicted by researchers. As an example, Shokrieh and Taheri-Behrooz [18] presented a new fatigue lifetime energy-based model for polymer composites. In another research [19-20], they conducted the fatigue simulation of laminates under cyclic loading conditions, based on the damage model, besides evaluating experimental data. Shabani et al. [21] introduced a progressive fatigue damage model for notched composite rings. Samareh-Mousavi et al. [22] performed a nonlinear finite element analysis to model the fatigue damage in laminates, under pin-loaded conditions.

Furthermore, although bones have been studied for decades, it is still an ongoing topic for scientists and researchers. Studies about predictions of the reliability and the scatter-band for the fatigue lifetime of bones are still rare. In this research, load-controlled fatigue tests of bovine tibia bones have been performed and then, predictions of the scatter-band and the reliability have been

conducted on experimental data. The reason for investigating the bovine bone in this research, instead of the human bone, was limits in providing human bones. As another note, Poumarat and Squire [23] concluded that human and fresh bovine samples presented a significantly different elastic modulus. However, depending upon their trabecular textures (dense or medium), the material behavior would be changed. In addition, the ultimate strength of bovine bones (8.5 ± 4.2 MPa) and human bones (8.78 ± 5.2 MPa) was almost the same [24]. Besides, the fatigue phenomenon should be considered, since the design of implants by engineers needs such knowledge about material properties. Therefore, the scatter-band properties and the reliability of implants for higher lifetimes, especially under cyclic loading should be studied. As a result, in this research, the analysis of the scatter-band and the reliability for bovine bones was done under cyclic loading. For this objective, fatigue testing was done by the rotary-bending fatigue machine, at different loading frequencies. Then, obtained results were presented in the figures and tables.

2. Materials and Experiments

In this research, the studied material was tibia bones of 12-month old cows. For standard test specimens, about 40 cylindrical samples were machined, which is shown in Fig 1. The diameter of standard specimens was 6 mm and the length of standard specimens was 76 mm. Measured diameters of samples were in the range of 5.787 ± 0.209 mm.

A device for rotating and bending fatigue testing was used, as is shown in Fig 2. Load-controlled fatigue testing was performed at loading levels, corresponding to 0.4 and 0.6 kg, based on measured real loading on bones, as was also reported in the literature [24].

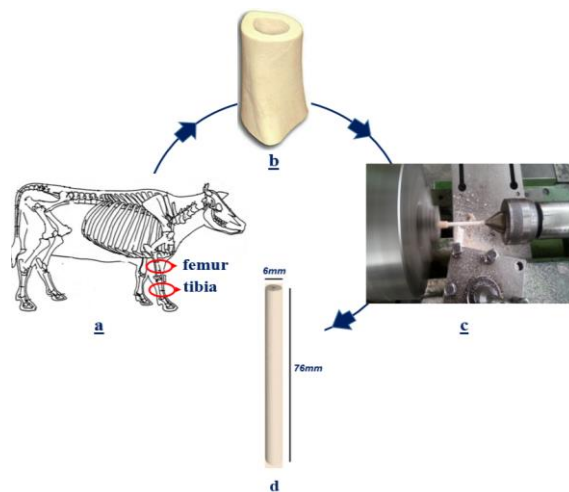


Fig. 1. Stages of the sample preparation, from (a) to (d)

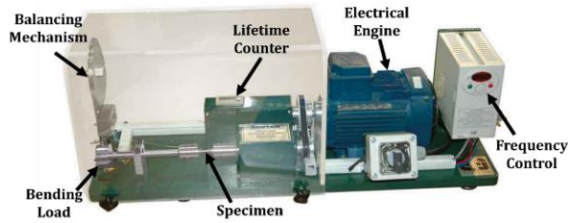


Fig. 2. The device for rotating bending fatigue testing

To verify such stress levels during fatigue testing, if the elastic modulus of bones was considered as 13-30 GPa [2]; then, the strain would be calculated between 1859 and 8141 micro-strain, by considering the weight of 0.4 and 0.6 kg. In the literature [24], the measured strain in bones was reported as 735-11850 micro-strain. These values demonstrated a proper agreement with considered stress levels in this research.

Fatigue testing was conducted under different loading frequencies, including 10, 20 and 30 Hz and repeated for 4 times at each stress level. Such loading frequencies had been considered in some references [9, 10, 13, 25]. Based on the literature, the loading frequency was mentioned from 0.5 to 125 Hz. For walking, the loading frequency may be measured as 1 Hz and for running, it should be higher. More details of testing could be observed in the previous research [2].

2.1. Statistical Predictions

The statistical analysis was important for the fatigue behavior of bones, since it could show the scatter-band and the reliability of experimental data. For the scatter-band prediction, three confidence levels were selected, as 85, 90, and 95%. Then, lower/upper bands were drawn for various target functions. This target function was introduced as the ratio of logarithmic fatigue lifetimes to stress levels, by the literature [2].

For analyzing the reliability, as the probability of survivals, a suitable probability function should be suggested. This model should be fitted to all data, at each stress level. In this research, three common distribution functions were considered, including normal, extreme maximum value (EMV) and smallest extreme value (SEV) distributions.

The probability density function (PDF), $F(t)$, was obtained based on the distribution function. Then, the cumulative distribution function (CDF), $F(t)$, could be calculated for failures. Then also, the reliability, $R(t)$, could be obtained for non-failures. In this research, t (the random variable) was the fatigue lifetime. The PDF specified the distribution of a failure through the fatigue lifetime and indicated the absolute failure speed [26-27]. Besides, the probability that a test sample would fail during an interval, $[0, t]$ was defined by the CDF.

For related formulations, the probability density function based on the normal distribution could be written as follows [26-27].

$$F(t) = \int_0^t f(t)dt \tag{1}$$

$$f(N) = \frac{1}{\sigma\sqrt{2\pi}} \exp \left[-\frac{(N - \mu)^2}{2\sigma^2} \right] \tag{2}$$

In which, μ and σ are the average value and the standard deviation of fatigue lifetimes (N), respectively.

The scatter-band could be found based on the average value and the standard deviation, such as $\mu=N\pm z\sigma$, where z is related to the confidence level. Its value was 1.44, 1.65 and 1.96 for 85, 90 and 95% of the confidence level [28]. Then, the cumulative distribution function could be written as follows [26-27].

$$F(N) = \frac{1}{2} \left[1 + \operatorname{erf} \left(\frac{N - \mu}{\sigma\sqrt{2}} \right) \right] \tag{3}$$

$$\operatorname{erf}(x) = \frac{1}{\sqrt{\pi}} \int_{-x}^x e^{-t^2} dt \tag{4}$$

To find the failure probability, the following relation could be utilized [26-27].

$$P = \min\{F(N)\} \times 100 \tag{5}$$

In addition, the probability could be obtained by the CDF, $R(t)$, entitled as "reliability" and it could be written as the following relation [26-27].

$$R(t) = 1 - F(t) \tag{6}$$

Probability functions of different distributions are shown in Table 1. In this table, μ is the location parameter (the mean value of experimental data at each stress level) and σ is the scale parameter (the variance of experimental data at each stress level). The function $\Phi(t, \mu, \sigma)$ indicates the standard normal CDF [26-27]. The value of mentioned parameters in distribution functions is denoted by rewriting PDFs in the form of the standard linear equations through a mathematical transformation: $Y = A + BT$ [26-27]. These linear equations of distribution functions with their variables, Y and T , are illustrated in Table 2. Values of A and B in all linear equations of distributions have been specified by following equations [26-27].

$$\hat{A} = \bar{Y} - B\bar{T} \tag{7}$$

$$\hat{B} = \frac{\sum_{i=1}^k (T_i - \bar{T})(Y_i - \bar{Y})}{\sum_{i=1}^k (T_i - \bar{T})^2} \tag{8}$$

The symbol "over-bar" denotes the average value and k is the total number of specimens in each stress level [26-27].

3. Results and Discussions

The first results, including lower/upper scatter-bands for a target function (the ratio of logarithmic fatigue lifetimes to stress levels), versus the loading frequency, can be seen in Figs 3 and 4, for 0.4 and 0.6 kg of the loading level, respectively. As a general result, by increasing the confidence level, the scatter-band became wider.

Table 1. Probability formula for different distribution functions

Distributions	$f(t)$	$F(t)$
Normal	$\frac{1}{\sqrt{2\pi}\sigma} e^{-\frac{(t-\mu)^2}{2\sigma^2}}$	$\Phi\left(\frac{t-\mu}{\sigma}\right)$
EMV	$\frac{1}{\sigma} e^{\left(\frac{t-\mu}{\sigma}\right)} e^{-\exp\left(-\frac{t-\mu}{\sigma}\right)}$	$e^{-\exp\left(-\frac{t-\mu}{\sigma}\right)}$
SEV	$\frac{1}{\sigma} e^{\left(\frac{t-\mu}{\sigma}\right)} e^{-\exp\left(-\frac{t-\mu}{\sigma}\right)}$	$1 - e^{-\exp\left(-\frac{t-\mu}{\sigma}\right)}$

Table 2. Linear equations of PDFs and variables of $Y = A + BT$

Distributions	Y	T
Normal	$\Phi^{-1}(F)$	t
EMV	$\ln\left(\ln\left(\frac{1}{F}\right)\right)$	t
SEV	$\ln\left(\ln\left(\frac{1}{1-F}\right)\right)$	t

On the other hand, obtained results for the scatter-band prediction at 0.4 and 0.6 kg indicated that by increasing the loading frequency, the scatter-band became narrower. At higher loading frequencies in composites, the temperature was increased due to the internal heat generation [29]. The reason could be the mismatch between thermal expansion coefficients of fibers and the matrix at elevated temperatures [30] and also friction between layers or fibers and the matrix at room temperature [29]. Therefore, it could be claimed that as the number of failure mechanisms extended [29], higher failure possibilities could be expected and then, a lower scatter-band would occur. Although the loading frequency had no significant effects on high-cycle fatigue properties of materials [31].

As can be observed, wider scatter-bands were obtained at lower stress levels [3, 31]. Such a statement could be made, when results in Figs. 3 and 4 were compared together. However, the change of the scatter-band was not significant, when the stress level changed. As another result, the confidence level of 95% could not cover all fatigue experimental data at 0.4 kg, due to scattered experimental data at all values of the loading frequency. Therefore, the confidence level should be increased for this case (more than 95%). However, all fatigue experimental data at 0.6 kg were covered by the confidence level of 90%.

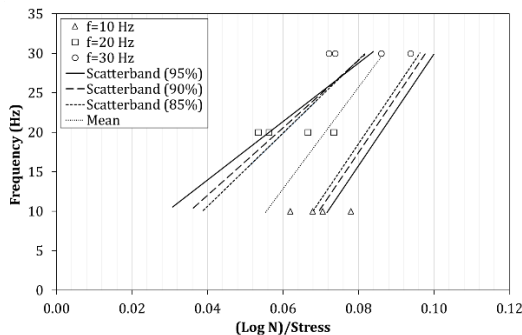


Fig. 3. The scatter-band for tibia bones under 0.4 kg of bending loading

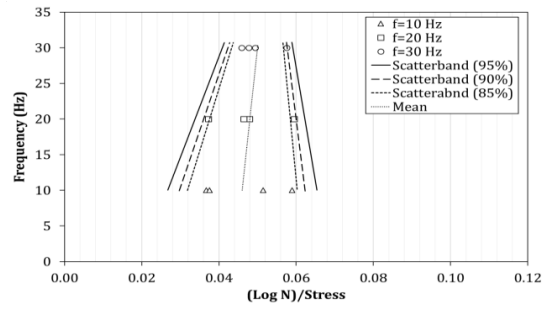


Fig. 4. The scatter-band for tibia bones under 0.6 kg of bending loading

Obtained results for the reliability prediction, are depicted in Figs. 5 to 10, including the CDF by three different distribution functions (normal, SEV and EMV distributions) for load-controlled fatigue lifetimes of tibia bones, under different loading frequencies and two bending stresses. For obtained CDF data, curve fitting was performed, besides showing the fitted equation and the coefficient of determination. As another result for the reliability prediction, the failure probability is reported in Tables 3 to 5, for different loading frequencies (10, 20 and 30 Hz) and various distribution functions.

As a first discussion for Figs 5 to 10, the coefficient of determination for all curve fittings was more than 99%, which showed proper modeling (utilizing a second-order equation). Then, by increasing the fatigue lifetime (or decreasing the stress level), the CDF value increased.

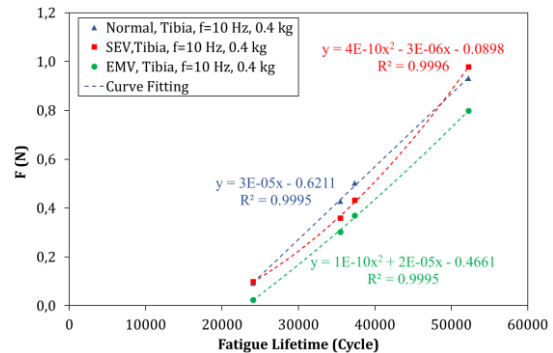


Fig. 5. The reliability prediction for tibia bones under 0.4 kg of bending loading, under the loading frequency of 10 Hz

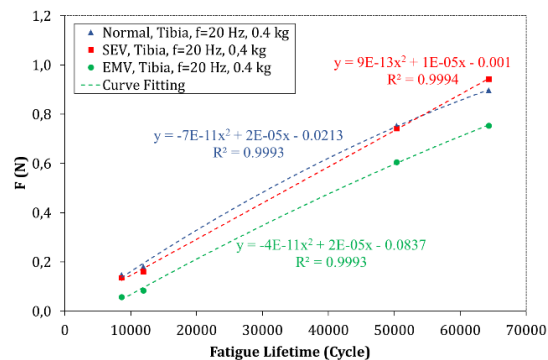


Fig. 6. The reliability prediction for tibia bones under 0.4 kg of bending loading, under the loading frequency of 20 Hz

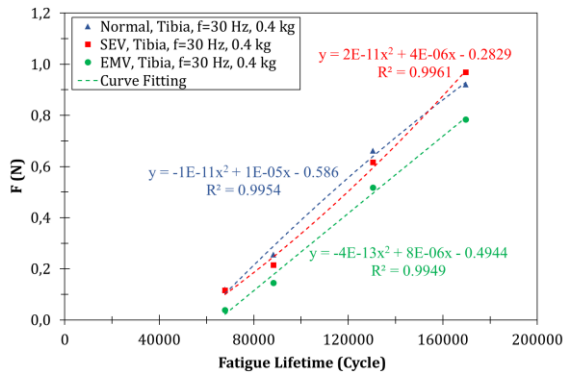


Fig. 7. The reliability prediction for tibia bones under 0.4 kg of bending loading, under the loading frequency of 30 Hz

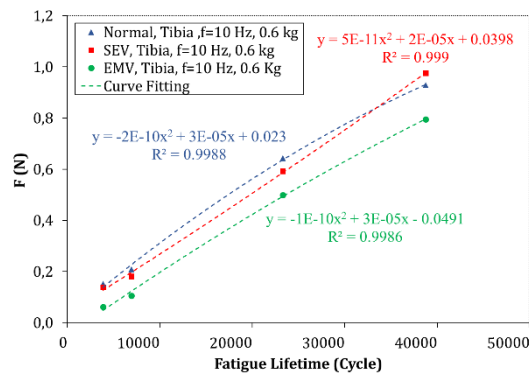


Fig. 8. The reliability prediction for tibia bones under 0.6 kg of bending loading, under the loading frequency of 10 Hz

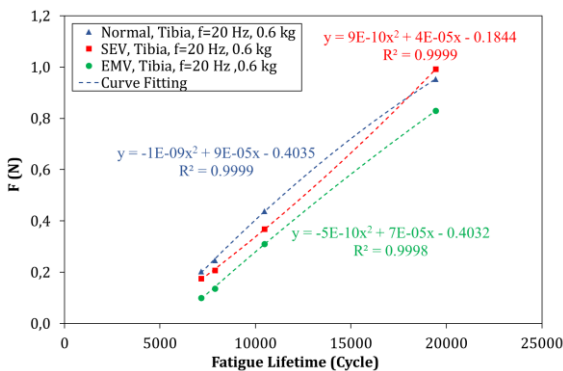


Fig. 9. The reliability prediction for tibia bones under 0.6 kg of bending loading, under the loading frequency of 20 Hz

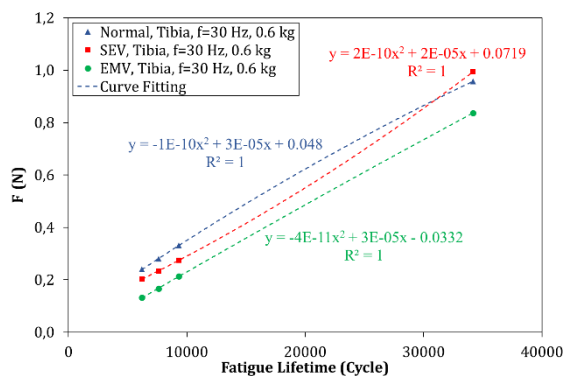


Fig. 10. The reliability prediction for tibia bones under 0.6 kg of bending loading, under the loading frequency of 30 Hz

Such results were also reported by Paquet et al. [32] for the high-cycle fatigue behavior of stainless steels. In addition, Jamalkhani Khameneh and Azadi [27] reported that the CDF value enhanced, when the stress level increased at a constant fatigue lifetime. However, the reliability decreased during high-cycle fatigue testing for cast iron. Therefore, it could be claimed that there was a good agreement between presented results for metals in the literature [27, 32] and obtained results for bones in this research.

Generally, using the normal distribution function, higher CDF values were obtained. The lowest value for the CDF was calculated based on the EMV distribution function. It should be noted that Jamalkhani Khameneh and Azadi [27] claimed that the best distribution function for high-cycle fatigue properties of cast iron was the normal function, after the three-parameter Weibull distribution function. They evaluated different distribution functions to find superior function for cast iron.

For the failure probability in Tables 3-5, it could be concluded that by increasing the loading frequency, the probability increased at 0.6 kg of the bending stress. However, this behavior was not seen for 0.4 kg. The reason could be observed in Fig 3, where some fatigue lifetimes had lower values at 20 Hz of the loading frequency, in comparison to those at other loading frequencies. At each loading frequency, the probability at 0.6 kg was higher than that of 0.4 kg. Such a result was also reported by Taylor [11], which showed a good agreement with obtained results in this article.

Table 3. The failure probability for the normal distribution

Loading	Frequency (Hz)	Probability (%)
0.6 kg	10	15.21
	20	20.23
	30	24.02
0.4 kg	10	9.35
	20	14.78
	30	11.93

Table 4. The failure probability for the SEV distribution

Loading	Frequency (Hz)	Probability (%)
0.6 kg	10	13.95
	20	17.54
	30	20.31
0.4 kg	10	9.01
	20	13.65
	30	11.65

Table 5. The failure probability for the EMV distribution

Loading	Frequency (Hz)	Probability (%)
0.6 kg	10	6.11
	20	10.01
	30	13.19
0.4 kg	10	2.37
	20	5.81
	30	3.88

By using the MINITAB software, a sensitivity analysis was done to find the effect of loading and frequency on the probability percentage. More details for such evaluation could be observed in the literature [2, 33-35]. It should be noted that the objective function was considered as follows,

$$P = C_1L + C_2F + C_3LF \quad (9)$$

where P was the probability, L was loading and F was the frequency. By this function, the coefficient of determination was higher than 98.6%. Besides, the highest P-Value for the regression analysis was 0.003. Since this value was lower than 0.05 (according to consider 95% for the confidence level), the regression analysis was meaningful for the reliability by three distribution functions and the objective function was proper.

Based on obtained results from the regression analysis, it could be concluded that for normal and SEV distributions, the loading parameter (with the P-Value lower than 0.05) was a sensitive factor on the probability. However, the frequency and the interaction between the two parameters were not effective. For the EMV distribution, loading and frequency had no effect on the probability of results. Moreover, the interaction between the two parameters was an effective factor, with the P-Value of 0.021.

Moreover, obtained results showed that, the reliability prediction and the scatter-band analysis on fatigue experimental data of bones, could be significant values for engineers, where the fatigue lifetime could be found at any value of the reliability for bones to design reliable implants, as a substitution for bones. Another benefit of these results for designers was finding an estimation of the required warranty period of implants, compared to bones [27].

4. Conclusions

In this article, the load-controlled fatigue behavior of bovine tibia bones, as composite materials, has been investigated under various loading frequencies, for predictions of the reliability and the scatter-band. Obtained results could be described as follows,

- The scatter-band prediction had different behaviors at 0.4 and 0.6 kg, by increasing the loading frequency.
- The CDF value increased by increasing the fatigue lifetime. Besides, the highest value for the CDF was obtained by the normal distribution function and the lowest value for the CDF was calculated by the EMV distribution function.
- When the loading frequency increased, the probability increased too, at 0.6 kg of the bending stress. However, there was no such usual behavior for 0.4 kg.

According to the sensitivity analysis, only loading was effective on the probability for normal and SEV distributions. However, only the interaction between loading and the frequency affected the probability of the EMV distribution.

Nomenclature

μ	Average value of fatigue lifetimes
σ	Standard deviation of fatigue lifetimes
N	Fatigue lifetime
z	A parameter that is related to the confidence level
$R(t)$	Reliability
$f(t)$	Probability density function
$F(t)$	Cumulative distribution function

References

- [1] Piekarski K. Analysis of bone as a composite material. *International Journal of Engineering Science* 1973; 11(6): 557-565.
- [2] Azadi M, Farzannasab M. Evaluation of high-cycle fatigue behavior in compact bones at different loading frequencies. *Meccanica* 2018; 53: 3517-3526.
- [3] Zhai JM, Li XY. A methodology to determine a conditional probability density distribution surface from S-N data. *International Journal of Fatigue* 2012; 44: 107-115.
- [4] Lee YL, Pan J, Hathaway R, Barkey M. **Fatigue testing and analysis**. 1st ed. 2004.
- [5] Metallic materials. **Fatigue testing statistical planning and analysis of data**. Standard No. ISO 12107, ISO International Standard 2017.
- [6] Carpinteri A, Berto F, Fortese G, Ronchei C, Scorza D, Vantadori S. Modified two-parameter fracture model for bone. *Engineering Fracture Mechanics* 2017; 174: 44-53.
- [7] Kruzic JJ, Ritchie RO. Fatigue of mineralized tissues: Cortical bone and dentin. *Journal of the Mechanical Behavior of Biomedical Materials* 2008; 3-17.
- [8] Tanner KE, Wang JS, Kjellson F, Lidgren L. Comparison of two methods of fatigue testing bone cement. *Acta Biomaterialia* 2010; 6(3): 943-952.
- [9] Swanson SAV, Freeman MAR, Day WH. The fatigue properties of human cortical bone. *Medical and Biological Engineering* 1971; 9(1): 23-32.
- [10] Carter DR, Hayes WC, Schurman DJ. Fatigue life of compact bone - II. Effects of microstructure and density. *Journal of Biomechanics* 1976; 9(4): 211-218.
- [11] Taylor D. Fatigue of bone and bones: An analysis based on stressed volume. *Journal of Orthopaedic Research* 1998; 16(2): 163-169.
- [12] Carter DR, Caler WE. Uniaxial fatigue of human cortical bone. The influence of tissue

- physical characteristics. *Journal of Biomechanics* 1981; 14(7): 461-470.
- [13] Turner CH, Wang T, Burr DB. Shear strength and fatigue properties of human cortical bone determined from pure shear tests. *Calcified Tissue International* 2001; 69(6): 373-378.
- [14] Klemenc L, Fajdiga M. Estimating S-N curves and their scatter using a differential anti-stigmery algorithm. *International Journal of Fatigue* 2012; 43: 90-97.
- [15] Rathod V, Yadav OP, Rathore A, Jain R. Reliability-based design optimization considering probabilistic degradation behaviour. *Quality and Reliability Engineering International* 2012; 28(8): 911-923.
- [16] Schijve J. Statistical distribution functions and fatigue of structures. *International Journal of Fatigue* 2005; 27(9): 1031-1039.
- [17] Kobayashi Y, Satoh K, Kanamori D, Mizutani H, Fugii N, Aizawa T, Toyashi H, Yamada H. Evaluating the exposure dose of 320-row area detector computed tomography and its reliability in the measurement of bone defect in alveolar cleft. *Journal of Oral and Maxillofacial Surgery, Medicine, and Pathology* 2017; 29(4): 350-357.
- [18] Shokrieh MM, Taheri-Behrooz F. A unified fatigue life model based on energy method. *Composite Structures* 2006; 75: 444-450.
- [19] Shokrieh MM, Taheri-Behrooz F. Progressive fatigue damage modelling of cross-ply laminates, I: Modelling strategy. *Journal of Composite Materials* 2010; 44(10): 1217-1231.
- [20] Taheri-Behrooz F, Shokrieh MM. Progressive fatigue damage modelling of cross-ply laminates, I: Experimental evaluation. *Journal of Composite Materials* 2010; 44(10): 1261-1277.
- [21] Shabani P, Taheri-Behrooz F, Maleki S, Hasheminasab M. Life prediction of a notched composite ring using progressive fatigue damage models. *Composites Part B* 2019; 165: 754-763.
- [22] Samareh-Mousavi SS, Mandegarian S, Taheri-Behrooz F. A nonlinear FE analysis to model progressive fatigue damage of cross-ply laminated under pin-loaded conditions. *International Journal of Fatigue* 2019; 119: 290-301.
- [23] Poumarat G, Squire P. Comparison of mechanical properties of human, bovine bone and a new processed bone xenograft. *Biomaterials* 1993; 14(5): 337-340.
- [24] Cristofolini L. In vitro evidence of the structural optimization of the human skeletal bones. *Journal of Biomechanical Engineering* 2015; 48(5): 787-796.
- [25] Lafferty JF, Raju PVV. The influence of stress frequency on the fatigue strength of cortical bone. *Journal of Biomechanical Engineering* 1979; 101(2): 112-113.
- [26] Yang G. **Life cycle reliability engineering**. John Wiley and Sons, USA, 2007.
- [27] Jamalkhani Khameneh M, Azadi M. Reliability prediction, scatter-band analysis and fatigue limit assessment of high-cycle fatigue properties in EN-GJS700-2 ductile cast iron. *MATEC Web Conference* 2018; 165: 10012.
- [28] Jamalkhani Khameneh M. Evaluation of high-cycle bending fatigue behavior in EN-GJS700-2 ductile cast iron of crankshafts. BSc. Thesis, Semnan University, 2017.
- [29] Steahler JM, Mall S, Zawada LP. Frequency dependence of high-cycle fatigue behavior of CVI C/SiC at room temperature. *Composites Science and Technology* 2003; 63: 2121-2131.
- [30] Mall S, Engesser JM. Effects of frequency on fatigue behaviour of CVI C/SiC at elevated temperature. *Composites Science and Technology* 2006; 66: 863-874.
- [31] Stephens RI, Fatemi A, Stephens RR, Fuchs HO. **Metal fatigue in engineering**. John Wiley and Sons, USA, 2001.
- [32] Paquet D, Lanteigne J, Bernard M, Baillargeon C. Characterizing the effect of residual stresses on high cycle fatigue (HCF) with induction heating treated stainless steel specimens. *International Journal of Fatigue* 2014; 59: 90-101.
- [33] Khisheh S, Khalili K, Azadi M, Zaker Hendobadi V. Heat treatment effect on microstructure, mechanical properties and fracture behaviour of cylinder head aluminium-silicon-copper alloy. *The Journal of Engine Research* 2018; 50: 55-65.
- [34] Safarloo S, Loghman F, Azadi M, Azadi M. Optimal design experiment of ageing time and temperature in Inconel-713C superalloy based on hardness objective. *Transactions of the Indian Institute of Metals* 2018; 71(7): 1563-1572.
- [35] Azadi M, Iziy M, Marbout A, Azadi M, Hajiali Mohammadi A. Optimization of solution temperature and time in nickel-based superalloy of engine turbocharger based on hardness by design of experiments. *The Journal of Engine Research* 2016; 43: 63-71.